

Investigation of microstructural changes of ODS steel EP450 after Helium implantation

I Bartošová^{1,2}, M Dománková³, F A Selim² and V Slugeň¹

¹ Institute of Nuclear and Physical Engineering, Slovak University of Technology in Bratislava, Ilkovičova 3, 812 19 Bratislava, Slovak Republic

² Department of Physics, Bowling Green State University, 104 Overman Hall, OH 43403, USA

³ Department of Materials Science, Faculty of Materials Science and Technology in Trnava, Slovak University of Technology in Bratislava, Paulínska 16, 917 24 Trnava, Slovak Republic

E-mail: iveta.bartosova@stuba.sk

Abstract. Oxide dispersion strengthened steels (ODS) are good candidates for the first wall of the actual proposed nuclear fusion reactors. This work focuses on the investigation of EP450 ODS by Positron annihilation lifetime spectroscopy (PALS) and Transmission electron microscopy (TEM) in “as received” state and after Helium implantation. Helium implantation produces radiation damage which in many respects is similar to the one related to neutron irradiation. Additionally, the selected area electron diffraction (SAED) together with TEM revealed the nature of Y_2O_3 particles and identified chromium-rich carbides $M_{23}C_6$ in the base material. Positron measurements indicate a high concentration of small-scale defects distributed in the sample. TEM was used for identification of microstructural changes after Helium implantation.

1. Introduction

Oxide dispersion strengthened steels are promising materials for advanced nuclear systems. In fission reactors as well as fusion technologies the envisioned environment is much more severe. Therefore these steels will have to endure higher temperatures, doses and -for example- high corrosion in the Super-critical pressurized water reactor [1, 2]. The main advantage of ODS steels is their excellent high temperature strength. At present time, steel EP450 is used for wrapper tubes of reactors BN-600 and BOR-60 [3]. The microstructure of ODS is enhanced by dispersed particles of Y_2O_3 which influence dislocation movement. In positron measurements these particles act as trapping sites for positrons due to high positron affinity of Yttrium as was shown in previous work [4]. Therefore PALS can specifically probe the microstructure around Y_2O_3 particles.

In this work we study the behaviour of yttria oxide particles in as-received and helium-implanted samples. Helium implantation often serves as a certain simulation of irradiation damage [5] as neutron irradiation inside a nuclear reactor is not always available. This method allows one to avoid difficulty associated with high level of radioactivity that makes sample handling very difficult.



2. Experimental

The chemical composition of ODS ferritic steel used in this study is given in table 1. Special care has been paid to prepare samples for TEM measurements. Since the implantation depth is only about 1 μ m from the surface we had to modify the sample preparation. The kinetic energy of ^{2+}He ions reached 500keV, achieving irradiation induced damage roughly 10 dpa, which is relative to 0.1C/cm². Temperature during implantation of ^{2+}He ions into the samples was about 52-60°C.

Table 1. Chemical composition of EP450 ODS steel [3].

Element	Fe	Cr	V	Ti	C	Si	Mn	Mo	Ni	Nb	Y ₂ O ₃
Wt.%	83,24	13.1	0.18	0.25	0.13	0.23	0.44	1.61	0.12	0.35	0.35

2.1 Positron annihilation lifetime spectroscopy measurements

A standard positron source ^{22}Na deposited on a Kapton foil was used. The estimated positron source activity is about 1MBq. We applied a sandwich setup in which two identical samples cover the source to achieve higher statistics. Each spectrum contained at least 1×10^6 counts and was evaluated with PATFIT'88 program [6]. Decay components due to annihilation in NaCl ($\approx 430\text{ps}$) and kapton foil ($\approx 382\text{ps}$) were subtracted in the procedure.

2.2 Transmission electron microscopy and selected area electron diffraction

In the case of as-received sample, a thin steel foil with thickness of 0.1mm was prepared by mechanical grinding. Afterwards targets with 3mm diameter were further thickened in Tenupol 5 device in a solution of: 300 ml HNO₃ + 700 ml CH₃OH, voltage 15V and electrolyte temperature 0°C. After cleansing in ethanol and drying, the sample was prepared for TEM.

As mentioned above, the preparation procedure of the thin foil of the implanted sample was modified. For the final thinning process ion bombardment of accelerated Argon particles was used. The acceleration voltage was 5kV, maximum current 2.5A and preparation time 15 hours.

Investigations by TEM were carried out on JEOL 200CX electron microscope with accelerating voltage 200 keV. SAED for identification of lattice parameters supplemented TEM analyses.

3. Results

3.1 TEM results

Figures 1 and 2 show TEM images for the sample before Helium implantation. Figure 1 shows non-uniform distribution of quasi-globular particles in ferritic matrix. Size and pattern of segregated globular particles is strongly heterogenic. The particles size and distribution were evaluated from TEM images. The size varied from 5 to 450 nm. Almost 60% of all particles were in the 20-40nm range. These particles were identified by SAED as particles of Y₂O₃. Aside from Ytria particles also particles of irregular shape were observed. These particles precipitate mainly on ferritic grain boundaries and were identified as M₂₃C₆ carbides as can be seen in figure 2. Presence of these carbides is a result of the chemical composition; however they do not have a beneficial effect on the microstructure.

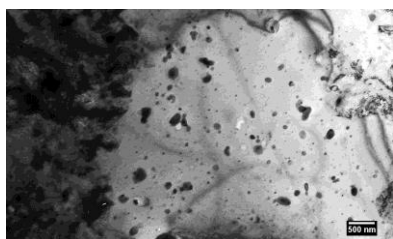


Figure 1. *Before implantation:* Dispersed particles (Y₂O₃ oxides) of quasi-globular shape in ferritic matrix.

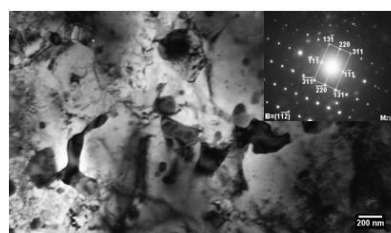


Figure 2. *Before implantation:* Detail on M₂₃C₆ particles of irregular shape precipitating on ferritic grain boundaries.

Figures 3-6 represent the sub-structure of the Helium implanted sample. The matrix is composed of ferrite, which retained its polyedric morphology. In comparison to the as-received state we are able to observe increased density of dislocations in the surface layer. Also a decrease in overall Yttria particle density was observed in comparison to as-received state. The particles are still arranged heterogeneously and their size ranged from 4-200 nm, however the dominant size is still 20-40 nm.

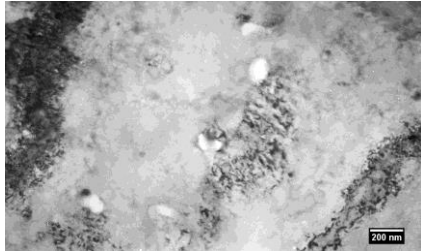


Figure 3. *After implantation:* Detail on sporadic occurrence of fine Y_2O_3 particles in ferritic matrix.



Figure 4. *After implantation:* Ferritic grain with needle shaped particles.

Fine needle shaped particles can be also observed in the ferritic matrix (figures 4, 5). From the nature of these particles behaviour, we can assume the formation of coherent aggregations of alloying elements, which probably conjoined by the influence of the implantation. These aggregations segregate in the ferritic matrix in a very homogenic manner and they also preserve their preferential orientation. From analyses of the diffraction spectrum, we conclude that the nature of segregation is related to the $\{211\}$ type habitual plane of ferrite. In figure 6 we can also observe interactions of dislocations with fine globular particles of Yttria.



Figure 5. *After implantation:* Detail on needle shaped particle in ferritic matrix.

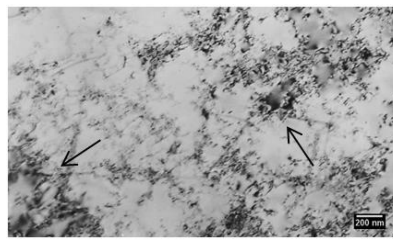


Figure 6. *After implantation:* Interaction of dislocations with fine yttria particles.

3.2 PALS results

PALS is based on the principle that electron–positron annihilation is time-dependent on the electron density in matter. If the metal contains defects such as vacancies, vacancy clusters and dislocations i.e., regions of less than average atomic density, positrons may become trapped at these defects [7, 8, 9]. The trapping of positrons into defects takes place in competition with the annihilation of the positrons in the bulk. Lifetimes τ_1 , τ_2 and intensities are shown in figure 7 and 8. The shorter component τ_1 represents the reduced lifetime, which is the bulk lifetime reduced by an amount that depends on positron trapping. The longer component τ_2 represents contribution of the positrons trapped at one or more type of defects. The second component τ_2 in as-received state is about 174ps. This lifetime corresponds to dislocations and/or mono-vacancies. Figure 8 suggests that 60% of positrons get trapped and annihilate at these sites. The average lifetime value was calculated using equation (1).

$$\tau_{avg} = \tau_1 I_1 + \tau_2 I_2 \quad (1)$$

The average lifetime τ_{avg} in “as-received state” is about 133ps. After Helium implantation both values of τ_2 and τ_{avg} rose. Lifetime of positrons in defects increased by ≈ 70 ps and the average lifetime by

25ps. This refers to formation of larger defects, i.e. vacancy clusters. The τ_2 value of 240ps probably corresponds to clusters of 3-vacancies in average, however also larger defects may be present in the samples due to the fact that Helium can occupy vacancies and therefore the defect appears smaller. The intensity of this long-lived component is about 40%. In fact the decrease of I_2 after He implantation (see Fig. 8) indicates that yttria oxide particles have filled some of the vacancies and open volume defects and prevented positron trapping. In figure 8 we can observe interactions of dislocations with Yttria particles. It is probable that dislocations also form around the needle shape particles and together with Y_2O_3 particles create attractive sites for positron trapping and annihilation.

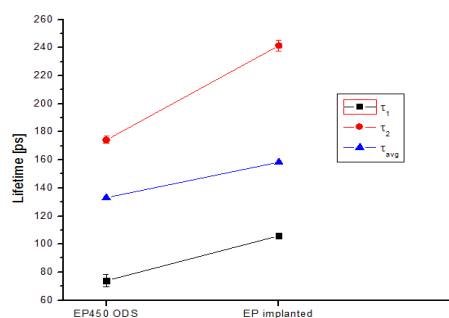


Figure 7. Reduced lifetime in bulk (τ_1) and defect (τ_2). Average lifetime (τ_{avg}) was calculated.

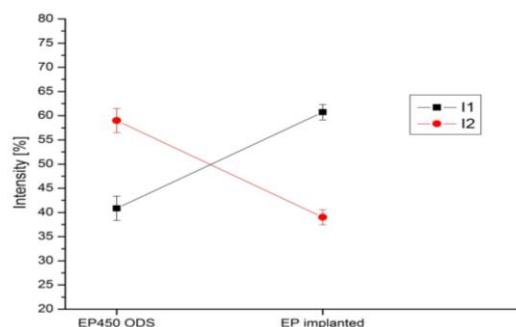


Figure 8. Intensities of lifetime components. Intensity I_1 , I_2 corresponds to τ_1 and τ_2 respectively.

4. Conclusion

EP450 ODS was studied by PALS and TEM in “as-received” state and after Helium implantation. After implantation we observed formation of needle shaped particles. These are probably clumps of alloying elements which formed due to the implantation effect. The re-localization of these elements produced larger vacancy clusters and dislocations. After Helium implantation Y_2O_3 particles became more sporadic and not visible by TEM technique. Therefore implantation also influences the state of Y_2O_3 particles. In this case we observed that Yttria particles became finer and their amount decreased in comparison to “as-received” state. PALS revealed clusters of 3-vacancies, however also larger defects may be also present in the samples.

References

- [1] Novotny R, Janíka P, Penttilä S, Hähner P, Macák J, Siegl J, Hausil P 2013 *J. Of Supercritical Fluids* **81** 147
- [2] Jian Li, Zheng W, Penttilä S, Liu P, Woo O T, Guzonas D 2014 *J.Nucl.Mat* **454** 7
- [3] Nikitina A A, Ageev V S, Chukanov A P, Tsvelev V V, Porezanov N P, Kruglov O A 2012 *J.Nucl.Mat.* **428** 117
- [4] Bartošová I, Čížek J, Lukáč F, Slugeň V 2014 *Acta Phys. Pol. A* **125** 702
- [5] Troeva T, Popova E, Staikova P, Nankova N, Yoshiieb T 2012 *J Phys: Conference series* **207** 012033
- [6] Kirkegaard P, Pedersen N J, Eldrup M, Risø National Laboratory, DK-4000 Roskilde, Denmark, 1989
- [7] Puska M J, Lanki P, Nieminen R M 1989 *J.Phys.:Condens. Matter* **1** 6081
- [8] Krause-Rehberg R, Leipner H: Positron Annihilation in Semiconductors, Springer-Verlag, 1999.
- [9] Hautajarvi P: Positrons in Solids, Springer-Verlag, Heidelberg, 1979.